1978

Thermodynamic and Acoustic Simulation of Positive Displacement Refrigeration Compressors

F. Scheideman

M. Schary

R. Singh

THERMODYNAMIC AND ACOUSTIC SIMULATION OF POSITIVE DISPLACEMENT REFRIGERATION COMPRESSORS

Frederick Scheideman
ILG Industries
2850 North Pulaski Road
Chicago, IL 60641

Michael Schary
Research Division
Carrier Corporation
Carrier Parkway
Syracuse, NY 13221

Rajendra Singh
Carlyle Compressor Company
P. O. Box 4803
Syracuse, NY 13221

1.0 INTRODUCTION

The science of mathematical modeling and simulation of positive displacement compressors has advanced tremendously in the last decade. A review of the previous work and details of mathematical models can be found in references [1 - 4].

The present paper presents a simulation approach which is conceptually similar to some earlier efforts [3 - 6], yet is more comprehensive, as it has been designed specifically for application to a variety of refrigeration compressor products. The major objectives are as follows: (i) to predict overall thermodynamic performance indices such as capacity, power consumption and energy efficiency ratio (EER), (ii) to predict the behavior of individual components such as valves and to identify the sources of energy loss, and (iii) to predict manifold pressure pulsations, muffler attenuation characteristics, etc. A further objective has been to keep the program user-oriented with minimum possible computational time and reasonable accuracy. Although it is difficult to construct the compressor model as a "black box", an attempt has been made to keep experimental inputs as few as possible, based upon the modeling experience of the authors.

2.0 MATHEMATICAL MODELS

Figure 1 shows schematically a representation of a single cylinder compressor. The shell of a welded/bolted hermetic compressor may be thought of as the control volume boundary with mass and energy flows crossing the boundaries. Pertinent thermodynamic variables internal to the control volume are shown in Figure 1. Refer to the Nomenclature for the identification of variables.

A mathematical model of a multicylinder compressor must account for cylinder interactions through kinematic phasing (ϕ) and manifold pulsations [6]; for example, in closely spaced cylinders with a common plenum, the pulsations are dynamically coupled. Uncoupled cylinders, however, can be approximated as single cylinders in parallel. Thus, a compressor with any arbitrary number of cylinders can be modeled as multiple single cylinders and/or a combination of twin cylinders.

The various mathematical models for a positive displacement compressor are as follows:

2.1 Motor Model

It is assumed that electric motor dynamic variations are negligible so that steady-state motor torque (τ) vs. speed (ω) and efficiency (η_M) data can be utilized.

$$\omega = C_{\omega o} + C_{\omega 1}\tau + C_{\omega 2}\tau^2 + \ldots \quad (1)$$

$$\eta_M = C_{\eta o} + C_{\eta 1}\tau + C_{\eta 2}\tau^2 + \ldots \quad (2)$$

where $C_{\omega i}$ and $C_{\eta i}$ are curve-fit coefficients and can be determined from the manufacturer's data. ω is assumed to be invariant during a cycle. Although this assumption may not be justifiable in the case of some high speed machines [4], it is felt that this approximate model is adequate for steady-state simulations.

2.2 Cylinder Process Model

Ideally, a first law of thermodynamics modeling approach should be followed for predicting cylinder processes; but because of the extremely high computational time required, the simpler polytropic model [3, 4] is used.

$$p_c(\theta)\left[\frac{V_c(\theta)}{m_c(\theta)}\right]^{n_o} = \frac{\bar{p}_{sv}}{\left(\bar{\rho}_{sv}\right)^{n_o}} \quad (3)$$

$V_c(\theta)$ can be obtained from the kinematic model of the running gear; e.g., for a slider crank mechanism:

$$V_c(\theta) = V_o + (\pi D^2/4)\left([R - L] + [R\cos\theta + (L^2 - [a R \sin\theta]^2)^{1/2}]\right) \quad (4)$$

For reference purposes, crank angle ($\theta = \omega t$) is considered zero at bottom dead center.

Refrigerant subroutines are linked to the cylinder process model for computation of other thermodynamic variables such as temperature, enthalpy, entropy, etc.

2.3 Leakage Model

An accurate cylinder model must account for leakage past the piston rings. Assuming it to be an isothermal process, instantaneous leakage mass flow rate $\dot{m}_\ell(\theta)$ is:

$$\dot{m}_\ell(\theta) = \left[\frac{2}{f}\,\frac{\pi D^2}{R_g T_u(\theta)\ell}\,\frac{b^3}{}\,(p_u^2(\theta) - p_y^2(\theta))\right]^{1/2} \quad (5)$$

where u and y denote upstream and downstream conditions for flow into and out of the cylinder. The friction factor f can be determined from the Reynolds' number.

2.4 Valve Fluid Flow Model

Flow through valve ports ($\dot{m}_v$) is assumed to be isentropic, quasi-static, and inertialess.

$$\dot{m}_v(\theta) = \rho_u(\theta)\, A_v(x) \left[2\,(h_u(\theta) - h_y(\theta))\right]^{1/2} \quad (6)$$

The above equation can be used for both suction and discharge ports and is solved using refrigerant property subroutines. The valve flow area $A_v(x)$ is a function of valve lift $x(\theta)$. For simple valving systems, potential flow theory [4, 7] can be used to determine $A_v(x)$; but for more complex systems, steady-flow laboratory tests are recommended.

Cylinder mass $m_c(\theta)$ in Eq. (3) is given as

$$m_c(\theta) = \int_o^\theta [\pm \dot{m}_{vs}(\theta) \mp \dot{m}_{vd}(\theta) \mp \dot{m}_\ell(\theta)]\, d\theta + V_o \bar{\rho}_{dv} \quad (7)$$

Note that backflow through valve ports is allowed in Eq. (7).

2.5 Valve Dynamics Model

From thermodynamic and acoustic performance viewpoints, valve motion can be adequately defined by its first mode of vibration [6]. (It is, however, not sufficient for valve stress calculations [4]). Thus, a valve can be treated as a single degree of freedom system with effective mass, stiffness (K), and damping (ζ) values suitable to the first mode:

$$\omega^2 \frac{d^2x}{d\theta^2} + 2\zeta\,\omega\Omega \frac{dx}{d\theta} + \Omega^2\,[x(\theta) - x_o] = [\Sigma F_v(\theta)/K]\;\Omega^2 + K\delta \quad (8)$$

where Ω is the first natural frequency of the valve. Ω and K can be determined by using either of the following methods: (i) finite element analysis: Ω from the valve dynamic and K from valve static analyses, (ii) experiment: valve can be mounted in a fixture which simulates boundary conditions; Ω and ζ can be evaluated from either free or forced vibrations of the valve; and K can be determined by applying a known load.

Eq. (8) accounts for the valve free lift (x_o) and pre-load ($K\delta$). $\Sigma F_v(\theta)$ is the algebraic summation of the cylinder and manifold pressure forces, such that the valve displacement $x(\theta)$ is:

$$0 \le x(\theta) \le x_{stop} \quad (9)$$

2.6 Suction Heat Transfer Model

Heat transferred to the suction gas $\dot{Q}_s$ is considered to come from: (i) discharge gas $\dot{Q}_{ds}$, (ii) motor $\dot{Q}_M$, (iii) cylinder $\dot{Q}_c$, and (iv) ambient $\dot{Q}_e$:

$$\dot{Q}_s = \dot{Q}_{ds} + \dot{Q}_M + \dot{Q}_c \pm \dot{Q}_e \quad (10)$$

In principle, $\dot{Q}_{ds}$ could be calculated in a rigorous incremental fashion, element by element. However, the present work, and also [8], has shown that a simple counterflow heat exchanger model is reasonably accurate.

$$\dot{Q}_{ds} = UA_{ds}\,(\bar{T}_d - \bar{T}_s) \quad (11)$$

where U is the overall heat transfer coefficient [9]. $\dot{Q}_M$ and $\dot{Q}_c$ can be considered proportional to the cylinder work (W_c). $\dot{Q}_e$ can be estimated from standard heat transfer coefficients [9].

Thus, the temperature rise of the suction gas (ΔT_s) is:

$$\Delta T_s = \dot{Q}_s / \dot{m}_s c_p \quad (12)$$

2.7 Manifold Pressure Drop Model

For computation of steady-state pressure drop (Δp) in suction and discharge manifolds, a cascade of flow elements can be constructed. For analysis purposes, most of these elements can be approximated as circular pipes. Standard formulations [9] can be used to compute Δp.

2.8 Manifold Pulsations Model

Conceptually, the overall pressure at any point in a compressor plenum can be treated as a sum of average pressure and oscillating pressure $p(\theta)$. For small amplitudes, $p(\theta)$ can be analyzed using acoustic plane wave theory [10].

The pulsations are treated in the frequency domain using the acoustic impedance approach [11]. Valve mass flow rate data, $\dot{m}_v(\theta)$, is converted into the frequency domain ($\tilde{\dot{m}}_v(n\omega)$) using discrete Fourier transform techniques where n is the harmonic index and ~ sign above a symbol indicates that it is a complex quantity. The volume velocity $\tilde{\dot{X}}(n\omega)$ is given as:

$$\tilde{\dot{X}}(n\omega) = \tilde{\dot{m}}_v(n\omega)/\rho \quad (13)$$

$\tilde{\dot{X}}(n\omega)$ should account for the kinematic coupling between cylinders 1 and 2 whose instantaneous crank angles are given as:

$$\theta_1 = \omega t \text{ and } \theta_2 = \omega t + \phi \quad (14)$$

The resulting oscillating pressure, $\tilde{p}_1(n\omega)$ and $\tilde{p}_2(n\omega)$ at the discharge valves and $\tilde{p}_a(n\omega)$ at any other point, such as an anechoic termination, are given as:

$$\begin{Bmatrix} \tilde{p}_1(n\omega) \\ \tilde{p}_2(n\omega) \\ \tilde{p}_a(n\omega) \end{Bmatrix} = \begin{bmatrix} \tilde{Z}_{11}(n\omega) & \tilde{Z}_{12}(n\omega) \\ \tilde{Z}_{21}(n\omega) & \tilde{Z}_{22}(n\omega) \\ \tilde{Z}_{a1}(n\omega) & \tilde{Z}_{a2}(n\omega) \end{bmatrix} \begin{Bmatrix} \tilde{\dot{X}}_1(n\omega) \\ \tilde{\dot{X}}_2(n\omega) \end{Bmatrix} \quad (15)$$

Where the acoustic impedance matrix $[\tilde{Z}(n\omega)]$ includes terms accounting for cylinder interactions. $[\tilde{Z}(n\omega)]$ is the fundamental dynamic property of a manifold and is uniquely related to the manifold geometry and gas conditions and can be computed by using acoustic transmission line formulations [10]. For details, refer to [11].

The frequency domain acoustic pressures $\tilde{p}(n\omega)$ can be converted to time domain $p(\theta)$ by using an inverse Fourier transform.

2.9 Thermal Performance Model

Capacity, power requirement, EER, and volumetric efficiency of a multicylinder compressor are given as follows:

(i) Capacity = $N \dot{m}_s(\theta)\, \omega\, (h_d' - h_s)$ (16)

where h_d' is the enthalpy of the saturated liquid at discharge pressure $\bar{p}_d$.

(ii) Power = $N\, \omega\, W_c/(2\pi\eta_M\eta_f)$ (17)

where W_c is the cyclic cylinder work:

$$W_c = \int_0^{2\pi} p_c(\theta)\, dV_c(\theta) \quad (18)$$

(iii) Coefficient of performance = capacity/power

$$= 2\pi\, \dot{m}_s(\theta)\, (h_d' - h_s)\, \eta_M\, \eta_f/W_c \quad (19)$$

EER is the coefficient of performance in Btu/w-hr units.

(iv) Volumetric efficiency =

$$\left(\int_0^{2\pi} \dot{m}_{sv}\, (\theta)\, d\,\theta\right)/2\pi\, RD^2\, \rho_s \quad (20)$$

3.0 COMPUTATIONAL MODEL

The simulation program is written using structured programming techniques. While all input, output, and logic functions are handled in the main program, mathematical models are located in subroutines. Figure 2 shows, in flow chart format, the basic features of the computational model.

Data are input in units familiar to the design engineer in order to facilitate understanding of modeling parameters. Then the main program is initialized at $\theta = 0$ and steps through an entire crank revolution with incremental crank angle ($\Delta\theta$) steps. Refrigerant subroutines are linked, and various instantaneous variables are computed every $\Delta\theta$, first for cylinder 1 and then for cylinder 2. Time averaged variables and frequency domain based variables are not computed until after each revolution is complete. More than one iteration is required to converge variables to a cyclic steady state, as shown in Table 1 for a typical compressor. The simulation always checks to ascertain whether the final iteration has been reached. Convergence is a necessary (but not sufficient) condition for program termination. If the final iteration is reached before power and mass flow rate have converged, an error message is printed and no further output will be generated. The number of iterations (ITER) is specified by the user in order to avoid costly non-converging runs and can be optimized for most design studies. The convergence of seven important compressor variables is shown in Table 1. Note that convergence was reached in the fifth iteration for mass flow and power, while the other variables converged by the third iteration. Convergence of pressure pulsations (not shown here) is determined by the convergence of the highest pressure magnitudes in the frequency domain [6].

The program is structured in such a fashion that a user has numerous analysis and output options available to him. This, in the authors' opinion, is a cost-effective procedure. The various analysis

TABLE 1: CONVERGENCE OF VARIABLES

Iteration I	Temperatures		Pressures		Motor Speed (rpm)	Mass Flow Rate $\dot{m}(t)$ (lbm/hr)	Power (Watts)
	T_{sv} (°F)	T_{dv} (°F)	$\bar{p}_{sv}$ (psia)	$\bar{p}_{dv}$ (psia)			
0	50	160	47.5	210.6	3450	308	1518
1	92	233	46.0	212.8	3532	304	2211
2	102	261	45.9	213.4	3507	312	2703
3	110	274	46.5	212.4	3534	240	2150
4	110	273	46.5	212.4	3534	241	2186
5	110	274	46.5	212.4	3534	240	2180
6	110	274	46.5	212.4	3534	240	2180

options include a choice between single cylinder or a two-cylinder simulation. This is necessitated by the fact that the computational time for a two-cylinder simulation is approximately three times that required for a single-cylinder simulation. The various output options include the following: (a) tabular summary of thermofluid performance indices, (b) instantaneous cylinder pressure and valve motions, (c) p-V diagram and various energy losses, (d) manifold cyclic pressure variations, frequency spectra at various locations, etc. All output is printed/displayed in units and precisions familiar to the user.

4.0 RESULTS

The simulation model has been verified by comparing it to both analogous laboratory tests and rating charts.

Figure 3 shows schematically the data acquisition and processing system used. It has been developed to facilitate simultaneous acquisition of pertinent compressor variables (recorded on a multi-channel FM tape recorder) and load stand conditions. Data processing, in real or delayed time, can be accomplished through two options as shown in Figure 3. Extensive use of digital techniques has improved speed, accuracy, and flexibility.

Refrigerant temperature at the suction valve, T_{sv}, is an important variable for precise computation of capacity and volumetric efficiency. Predicted values for T_{sv} are compared with measurements for a number of conditions in Table 2. Note the excellent agreement for all conditions shown.

Cylinder pressure, an important indicator of a correct cylinder process model, is displayed in Figure 4. The accuracy of the polytropic model described previously is demonstrated by the excellent agreement between computed and measured results. The slight discrepancies during suction and discharge may be attributed to incomplete fluid flow and structural descriptions of the valves.

Figure 5 shows discharge valve displacement $x_d(\theta)$. The agreement is considered excellent considering the fact that valve dynamic model is extremely simplified.

Discharge plenum pressure, $p_{dv}(\theta)$, as shown in Figure 6(a), is fairly typical of a two-cylinder compressor. Figure 6(b) shows a frequency spectrum of plenum pressure magnitudes, $p_{dv}(n\omega)$. From both Figures 6(a) and 6(b), it is seen that the magnitude predictions agree extremely well with measured values, especially for the dominant harmonics. Since phase prediction cannot be compared to the experiment in the frequency domain, it must be compared indirectly in the time domain (Figure 6[a]). Again, the agreement is extremely good, especially at lower harmonics which affect valve motion significantly. The slight magnitude and phase prediction discrepancies can be attributed to the difficulty in approximating irregular cavities with regular acoustic elements which can be modeled easily. Otherwise, experimental techniques must be used [12].

Pressure frequency spectrum at anechoic termination, $p_{da}(n\omega)$, is shown in Figure 7. Note the excellent agreement at the dominant second and fourth harmonics. Some discrepancies at the higher harmonics point out the difficulties in modeling realistic manifolds and mufflers; thus, the agreement must be considered excellent at the present state of the art.

The ability of the simulation model to predict absolute compressor performance levels is the final test of its usefulness as a design tool. Figure 8 shows agreement between computed and rated capacity and EER for a typical compressor where agreement index α is defined as:

$$\alpha = 100\left(\frac{\text{Simulated value - Rated value}}{\text{Rated value}}\right),\% \qquad (21)$$

In both cases, capacity and EER agreements are within 4%. Moreover, experimental studies have shown that design changes incorporated in a compressor can be predicted within similar accuracy limits.

5.0 CONCLUDING REMARKS

An overview of a computer simulation model for refrigeration compressors has been presented. Excellent agreement with measurements has been shown for various time and frequency domain variables and overall performance indices.

The authors feel that the present approach differs from other simulation efforts [3 - 6] in the following ways: (1) the present model is fairly comprehensive and traces accurately the time history of the refrigerant as it enters and leaves the shell; (2) unlike some other models [3 - 6], which use ideal

TABLE 2: COMPARISON OF RESULTS FOR SUCTION GAS TEMPERATURE AT THE VALVE, T_{sv}

	Condition			T_{sv}, °F	
	$\bar{P}_s$, psia	$\bar{P}_d$, psia	T_s, °F	Measured	Computed
1	42.9	274.6	65	120	119
2	47.5	210.6	65	104	109
3	90.7	311.5	65	90	90
4	90.7	210.6	65	83	83

gas properties, realistic thermodynamic properties are utilized here; (3) the present simulation incorporates a cost-effective, yet accurate, computational model with multiple analysis options; and (4) the program is user-oriented in both input and output data format.

Some of the mathematical models may not be sufficiently rigorous from a theoretical viewpoint because the basic philosophy here has been that it is more productive to analyze a real physical system approximately than to apply sophisticated theory to an idealized system. In this context, the authors feel that there is a need for further study in the following areas: heat transfer, effect of fluid flow on manifold pulsations, effect of two-phase refrigerant flows on valves and cylinder processes, etc.

NOMENCLATURE

Symbols

- A - area
- a - offset
- b - leakage
- C - constant
- c_p - specific heat
- D - piston diameter
- EER - energy efficiency ratio
- f - friction factor
- h - enthalpy
- I - iteration index
- ITER - number of iterations
- K - valve stiffness
- L - strap length
- ℓ - leakage length
- m - mass
- $\dot{m}$ - mass flow
- N - number of cylinders
- NCYL - program cylinder index
- n_o - polytropic index
- n - harmonic index
- p - pressure
- $\dot{Q}$ - heat transfer rate
- R - crank throw
- R_g - gas constant
- t - time
- U - overall heat transfer coefficient
- V - volume
- V_o - clearance volume
- W - Work
- $\dot{X}$ - volume velocity
- x - valve displacement
- x_o - free lift
- δ - valve spring preset
- ζ - valve damping coefficient
- η - efficiency
- θ - crank angle
- ρ - density
- τ - motor torque
- ϕ - crank phasing
- Ω - valve natural frequency
- ω - crank speed in rad./time

Subscripts

- 1: cylinder #1
- 2: cylinder #2
- a: anechoic
- c: cylinder
- d: discharge
- e: environment
- f: friction
- i: index
- ℓ: leakage
- M: motor
- s: suction
- u: upstream
- v: valve
- y: downstream

Superscripts

- $\bar{}$: nominal quantity
- $\sim$: complex quantity

REFERENCES

1. E. B. Qvale, W. Soedel, M. J. Stevenson, J. P. Elson, and D. A. Coates, "Problem Areas in Mathematical Modeling and Simulation of Refrigerating Compressors", ASHRAE Paper No. 2215, 1972.

2. R. Singh and W. Soedel, "A Review of Compressor Lines Pulsation Analysis and Muffler Design Research, Part I - Pulsation Effects and Muffler Criteria, Part II - Analysis of Pulsating Flows", Proceedings of 2nd Purdue Compressor Technology Conference, pp. 102 - 123, 1974.

3. W. Soedel, "Introduction to Computer Simulation of Positive Displacement Type Compressors", Short Course Text, Purdue University, 1972.

4. J. F. Hamilton, "Extensions of Mathematical Modeling of Positive Displacement Type Compressors", Short Course Text, Purdue University, 1974.

5. J. P. Elson and W. Soedel, "Simulation of the Interaction of Compressor Valves with Acoustic Back Pressures in Long Distance Lines", J. Sound Vib., 34(2), pp. 211 - 220, 1974.

6. R. Singh, E. Sandgren, K. Ragsdell, and W. Soedel, "Simulation of a Two-Cylinder Compressor for Discharge Gas Pressure Oscillation Prediction", ASME Paper No. 76-WA/FE-10, 1976.

7. F. F. Ehrich, "Some Hydrodynamic Aspects of Valves", ASME Paper No. 55-A-114.

8. C. Hiller, "Improving Heat Pump Performance via Compressor Capacity Control", Ph.D. Thesis, M.I.T., 1976.

9. W. M. Kays and A. L. London, "Compact Heat Exchangers", McGraw Hill, New York, 1964.

10. S. N. Rschevkin, "A Course of Lectures on the Theory of Sound", MacMillan Co., New York, 1963.

11. R. Singh, "Modeling of Multicylinder Compressor Discharge Systems", Ph.D. Thesis, Purdue University, 1975.

12. M. Schary and R. Singh, "Compressor Manifold Acoustic Impedance Measurements Using Sine Sweep Excitation and Known Volume Velocity Technique", Purdue Compressor Technology Conference, 1978.

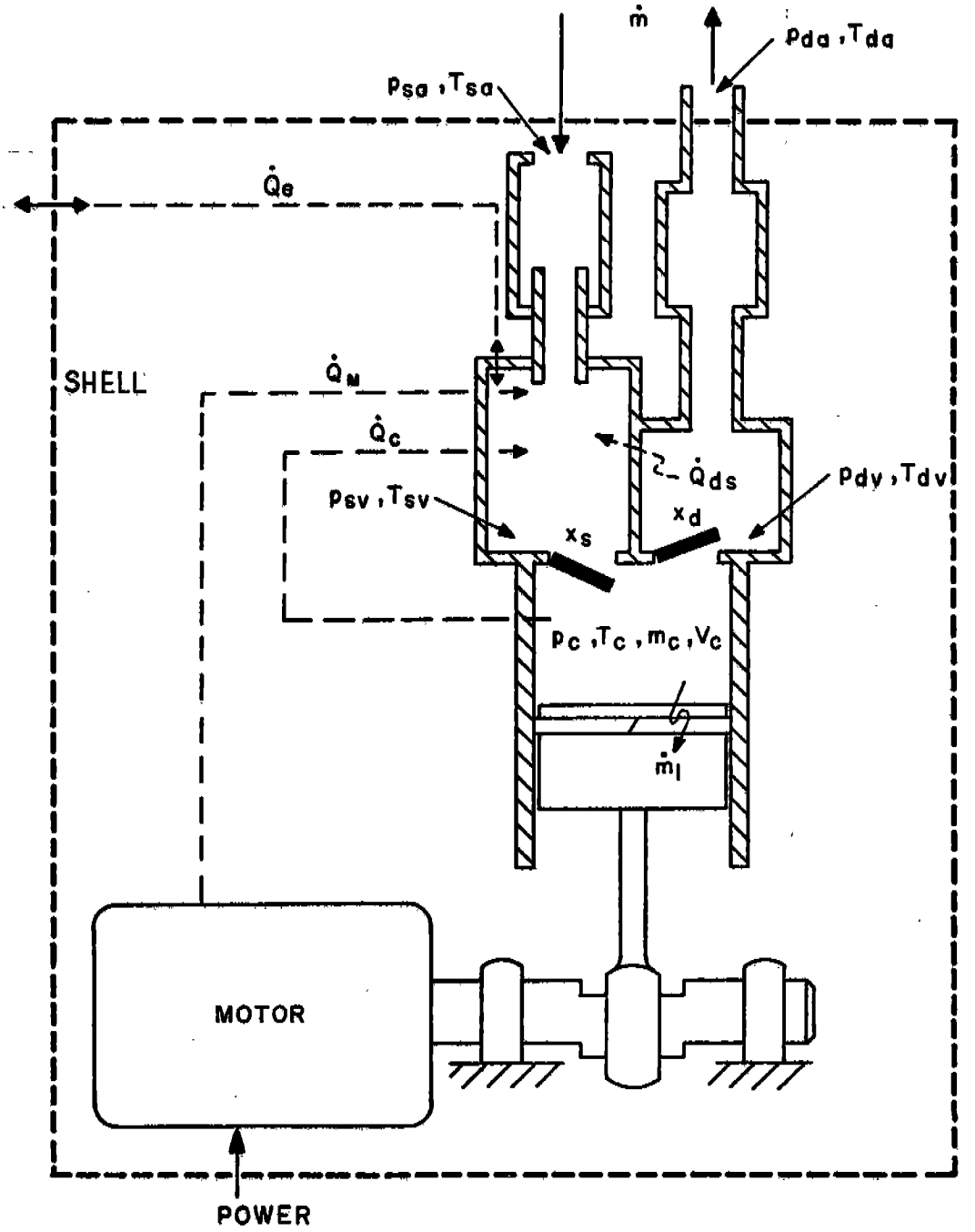

Figure 1. Schematic of Physical Model for a Single Cylinder Compressor

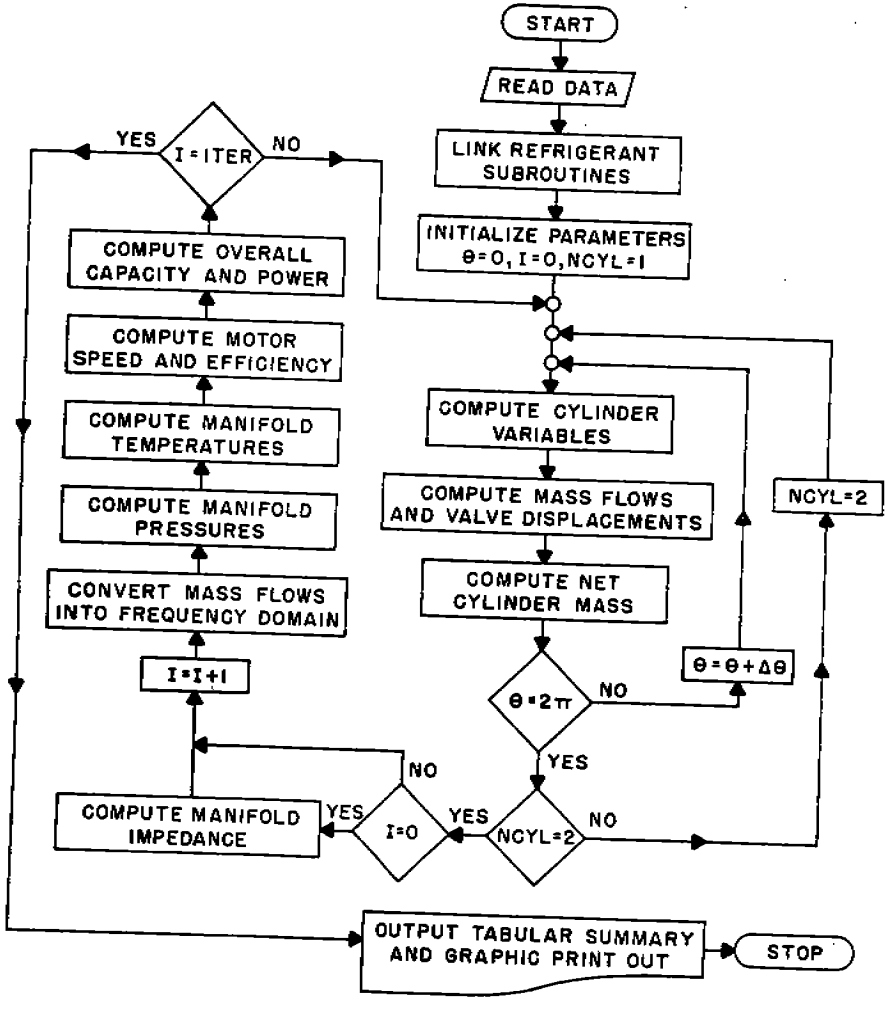

Figure 2. Flow Chart of Computational Model for a Two-Cylinder Compressor Simulation

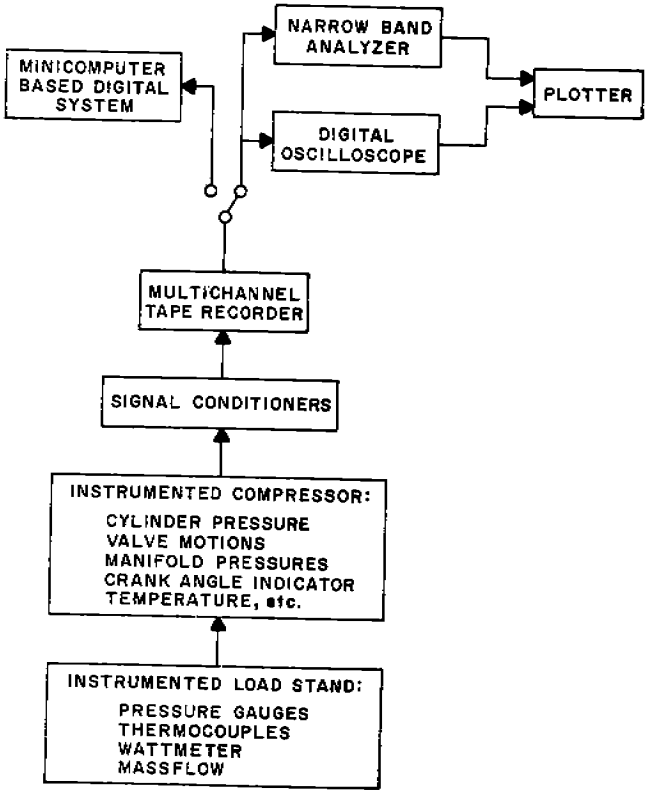

Figure 3. Schematic of Data Acquisition and Processing System

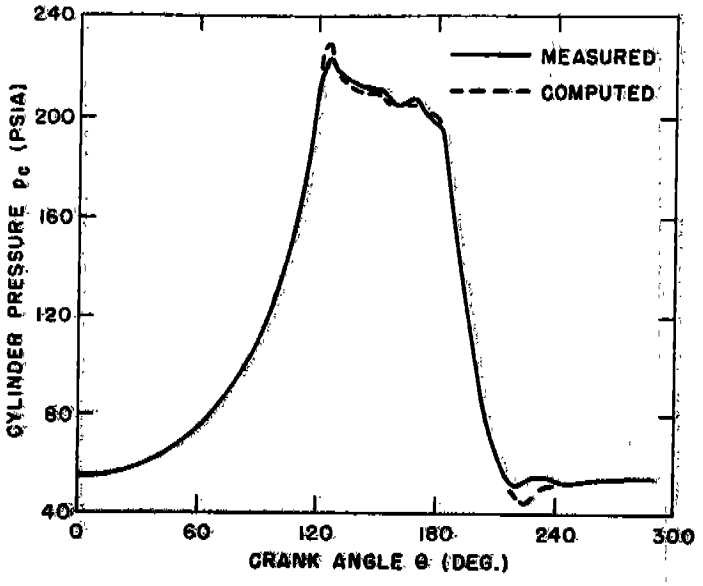

Figure 4. Cylinder Pressure $p_c(\theta)$

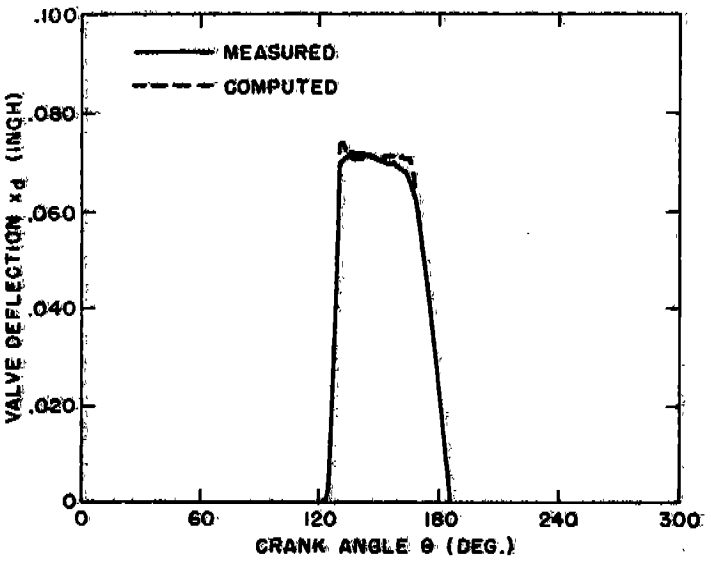

Figure 5. Discharge Valve Motion $x_d(\theta)$

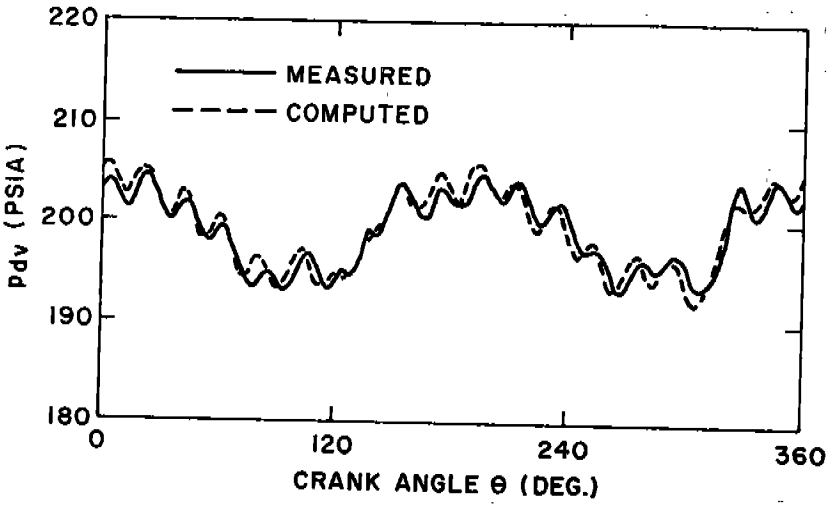

6(a)

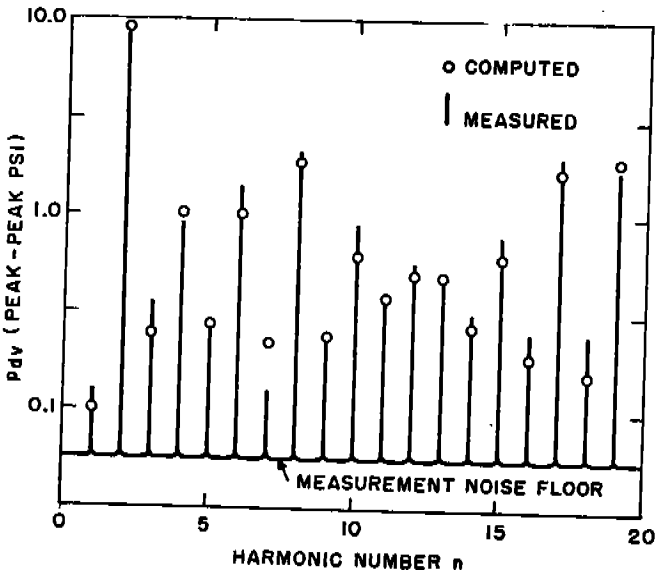

6(b)

Figure 6. Discharge Plenum Pressure p_{dv}.

(a) Cyclic Variation $p_{dv}(\theta)$.

(b) Frequency Spectrum $p_{dv}(n\omega)$.

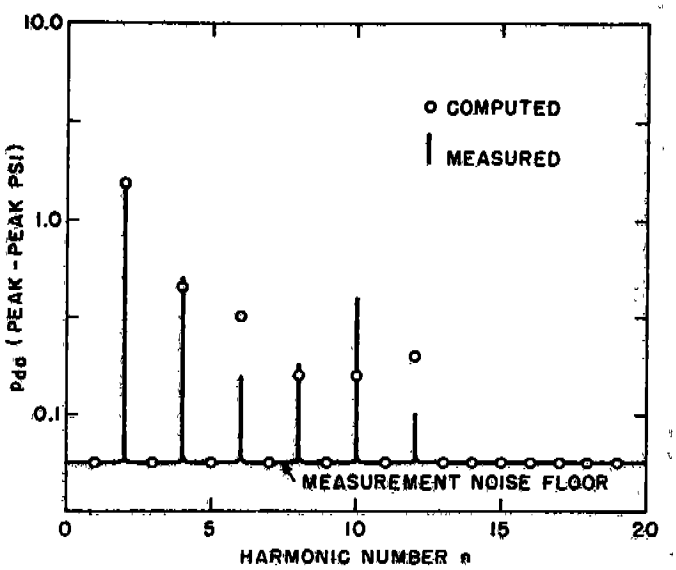

Figure 7. Pressure Frequency Spectrum at Anechoic Termination, $p_{da}(n\omega)$. Computational floor has been taken to be equal to the measurement noise floor.

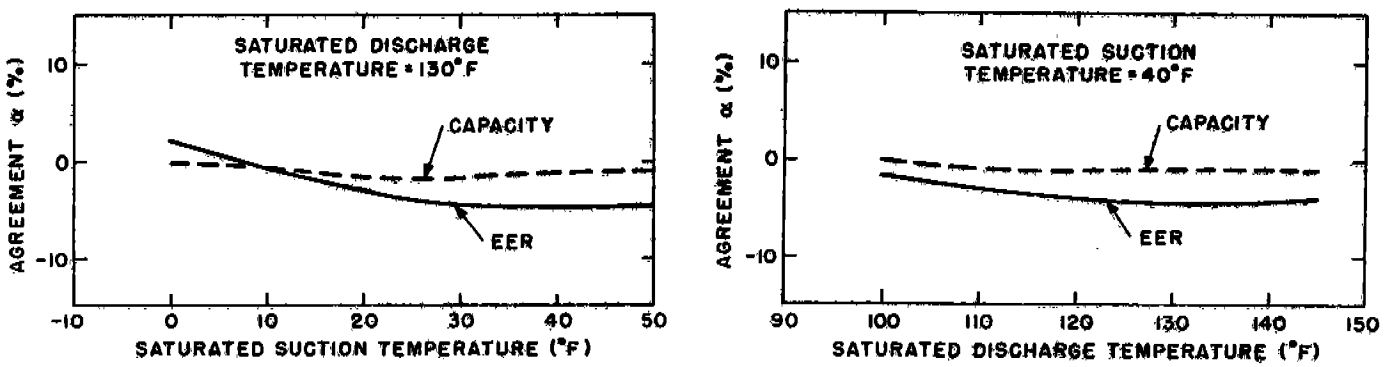

Figure 8. Agreement between Simulation and Rating Charts for Capacity and EER:
(a) at constant saturated discharge temperature, and
(b) at constant saturated suction temperature.